Redox Biology 26 (2019) 101288

Contents lists available at ScienceDirect

Redox Biology

journal homepage: www.elsevier.com/locate/redox

Increased mitochondrial NADPH oxidase 4 (NOX4) expression in aging is a causative factor in aortic stiffening

Chandrika Canugovi[a], Mark D. Stevenson[a], Aleksandr E. Vendrov[a], Takayuki Hayami[a], Jacques Robidoux[b], Han Xiao[c], You-Yi Zhang[c], Daniel T. Eitzman[a], Marschall S. Runge[a,**], Nageswara R. Madamanchi[a,*]

[a] 1150 West Medical Center Drive, 7200 Medical Science Research Building III, Department of Internal Medicine, Frankel Cardiovascular Center, University of Michigan, Ann Arbor, MI, 48109, USA

[b] 115 Heart Drive, Department of Pharmacology and Toxicology, The East Carolina Diabetes and Obesity Institute, East Carolina University, Greenville, 27834, North Carolina, USA

[c] Institute of Vascular Medicine, Cardiology Department, Peking University Third Hospital, NHC, Key Laboratory of Cardiovascular Molecular Biology and Regulatory Peptides, Key Laboratory of Molecular Cardiovascular Science, Ministry of Education, Beijing Key Laboratory of Cardiovascular Receptors Research, Beijing, 100191, China

A B S T R A C T

Aging is characterized by increased aortic stiffness, an early, independent predictor and cause of cardiovascular disease. Oxidative stress from excess reactive oxygen species (ROS) production increases with age. Mitochondria and NADPH oxidases (NOXs) are two major sources of ROS in cardiovascular system. We showed previously that increased mitochondrial ROS levels over a lifetime induce aortic stiffening in a mouse oxidative stress model. Also, NADPH oxidase 4 (NOX4) expression and ROS levels increase with age in aortas, aortic vascular smooth muscle cells (VSMCs) and mitochondria, and are correlated with age-associated aortic stiffness in hypercholesterolemic mice. The present study investigated whether young mice (4 months-old) with increased mitochondrial NOX4 levels recapitulate vascular aging and age-associated aortic stiffness. We generated transgenic mice with low (*Nox4*TG605; 2.1-fold higher) and high (*Nox4*TG618; 4.9-fold higher) mitochondrial NOX4 expression. Young *Nox4*TG618 mice showed significant increase in aortic stiffness and decrease in phenylephrine-induced aortic contraction, but not *Nox4*TG605 mice. Increased mitochondrial oxidative stress increased intrinsic VSMC stiffness, induced aortic extracellular matrix remodeling and fibrosis, a leftward shift in stress-strain curves, decreased volume compliance and focal adhesion turnover in *Nox4*TG618 mice. *Nox4*TG618 VSMCs phenocopied other features of vascular aging such as increased DNA damage, increased premature and replicative senescence and apoptosis, increased proinflammatory protein expression and decreased respiration. Aortic stiffening in young *Nox4*TG618 mice was significantly blunted with mitochondrial-targeted catalase overexpression. This demonstration of the role of mitochondrial oxidative stress in aortic stiffness will galvanize search for new mitochondrial-targeted therapeutics for treatment of age-associated vascular dysfunction.

Oxidative stress, mitochondrial dysfunction and aging are associated with the pathogenesis of cardiovascular diseases [1]. The two major reactive oxygen species (ROS) generating sources within cells are mitochondria and nicotinamide adenine dinucleotide phosphate (NADPH) oxidases (NOXs) [2,3]. Mitochondria generate ROS as a by-product of oxidative phosphorylation, while the major function of NADPH oxidases is generation of ROS. The NOX family members include NOX1-5 and DUOX1-2 isoforms [4]. Transmembrane NOX1, NOX2, NOX4, and NOX5 catalytic subunits are expressed in vascular tissue; however, NOX5 is absent in rodents [4]. All NOX subunits, with the exception of NOX5, interact with another transmembrane protein, p22phox, forming a membrane-bound catalytic core [5]. Unlike NOX1-3, NOX4 does not require conventional cytosolic regulatory subunits for activity, but DNA polymerase-δ-interacting protein 2 was shown to stimulate NOX4 activity in vascular smooth muscle cells (VSMCs) [6]. NOX4 activity is regulated at the expression level in response to a wide range of stimuli, generating predominantly H_2O_2, which can diffuse through membranes and affect intra- and intercellular signaling pathways [7–9]. Furthermore, NOX4 localizes to mitochondria, increasing mitochondrial ROS levels [10–12].

NOX4 is present in many cell types and is highly expressed in vascular wall cells [13]; its expression and activity are significantly increased in endothelial and smooth muscle cells in response to proinflammatory mediators and cytokines [14,15]. We recently showed that NOX4 expression is increased in VSMC mitochondria and vasculature and is associated with increased aortic stiffening and atherosclerosis in

* Corresponding author.
** Corresponding author.
E-mail address: madamanc@med.umich.ediu (N.R. Madamanchi).

https://doi.org/10.1016/j.redox.2019.101288
Received 5 June 2019; Received in revised form 9 July 2019; Accepted 29 July 2019
Available online 02 August 2019

aged hypercholesterolemic mice [12]. Furthermore, increased NOX4 expression in arterial wall in humans is correlated with age and atherosclerotic lesion severity [12,16].

Increased stiffness of large arteries, a major determinant of pulse pressure, is a significant and independent predictor of adverse cardiovascular events [17]. Conducting arteries such as aorta and carotid artery have large amount of elastin, allowing the vessel to expand and recoil to dampen the oscillatory changes in blood pressure arising from regular ventricular contractions [18]. The pressure waves, when reaching vascular branch points, are reflected back to the heart. In healthy individuals the reflected wave arrives during diastole, aiding in coronary blood flow; however, in individuals with aortic stiffening the pressure wave returns much quicker and arrives in systole, augmenting the afterload, inducing left ventricular hypertrophy, and reducing coronary blood flow. The resultant insufficiency in myocardial perfusion may cause myocardial ischemia and heart failure [19]. Furthermore, aortic stiffness is a precursor of hypertension [20].

Increased oxidative stress is implicated in decreased aortic compliance in patients with coronary artery disease [21]. We and others have shown that increased mitochondrial oxidative stress is a contributing factor in age-associated arterial stiffening [12,22,23]. However, it is not known whether mitochondrial oxidative stress plays a causative role in aortic stiffening. The present study was designed to determine whether increasing mitochondrial ROS production in young mice, by increasing NOX4 expression, would recapitulate the age-associated aortic stiffening observed by our laboratory and others. Our data demonstrate that increased mitochondrial oxidative stress in young mice induces aortic stiffening and VSMC phenotype similar to that observed in aged mice. Specifically, decreased aortic compliance with increased mitochondrial oxidative stress mainly results from structural remodeling of the vascular wall mediated by VSMCs rather than endothelial cells.

1. Results

Generation of Mitochondrial-specific Nox4 Transgenic Mice. The function of NOX4 in the pathogenesis of cardiovascular disease (CVD) is controversial. Some investigators reported that NOX4 provides protection against atherosclerosis [24] and cardiac dysfunction in response to pressure overload, particularly using young mice [25]. On the other hand, we and others showed association of increased NOX4 expression/activity with atherosclerosis [15,16,26] and cardiomyocyte hypertrophy, cell death, and cardiac fibrosis during pressure overload [27] and in cardiac remodeling [28]. In contrast to a report that NOX4 protein was not detectable in cardiomyocyte mitochondria under physiological conditions [29], at least 18 publications reported NOX4 localization to mitochondria in several cell types, including vascular cells, under pathophysiological conditions (for example [10–12]). We previously showed increased mitochondrial NOX4 expression in the aortic wall and VSMCs isolated from aortas with aging and its association with aortic stiffening and atherosclerosis in hypercholesterolemic mice [12].

Therefore, to determine whether increased mitochondrial NOX4 expression has a causative role in aging-associated aortic stiffness, we generated mitochondria-targeted *Nox4* transgenic (*Nox4*TG) mice with varying levels of *Nox4* expression, using a plasmid construct containing mouse *Nox4* gene (Fig. 1*A*). Southern analysis of genomic DNA identified a lower (TG605) and a higher (TG618) *Nox4* transgene containing founders (Fig. 1*B*). Gene expression analysis, measured by q-PCR, in VSMCs showed a 2-fold (*Nox4*TG605) and 20-fold (*Nox4*TG618) increase in *Nox4* mRNA levels relative to the wild-type (Fig. 1*C*). The *Nox4* expression in *Nox4*TG618 mice are in line with *NOX4* expression in aged human carotid arteries [12]. NOX4 protein expression in liver mitochondria was increased 2.1- and 4.9-fold in *Nox4*TG605 and *Nox4*TG618, respectively, compared with the wild-type (Fig. 1*D*). Further supporting the increased NOX4 mitochondrial localization in *Nox4*TG mice, a significant increase in yellow fluorescence was observed in VSMC mitochondria from the colocalization of MitoTracker Green FM and immunoreactive NOX4 (Fig. 1 *E* and *F*).

*Nox4*TG grew normally and did not show any gross phenotypic abnormalities. *Nox4*TG mice were not different from wild-type littermates in appearance, body weight (25.1 ± 0.76 vs 25.36 ± 1.15 g (mean ± SEM) wild-type littermates, ~4 months-old), behavior or fertility. The inheritance of *Nox4*TG allele in TG605 and TG618 mice was approximately 50% in accordance with Mendelian ratios, suggesting single chromosome integration of the transgene. *Nox4* transgene was expressed in all tissues studied. The expression of other NADPH oxidases– *Nox1* and *Nox2*– was not affected by *Nox4* transgene expression (data not shown).

Young *Nox4*TG Mice Phenocopy Age-associated Aortic Stiffening and Impaired Vasomotor Function. NOX4 is a critical mediator of increased mitochondrial oxidative stress during aging [12] and mitochondrial stress/dysfunction contributes to large elastic artery stiffening and impaired contractile function [12,22,23,30]. To determine whether young *Nox4*TG mice will recapitulate aging-associated vascular dysfunction, we first measured pulse wave velocity (PWV). Both young *Nox4*TG605 and TG618 mice (4 months-old) showed an increase in PWV, but the difference was not significant between *Nox4*TG605 and wild-type mice (Fig. 2*A*). However, PWV increased 4.5-fold in *Nox4*TG618 mice compared with age-matched wild-type mice (Fig. 2*A*). PWV was also significantly higher in *Nox4*TG618 mice compared with age-matched *Nox4*TG605 mice ($P < 0.05$). Vasomotor function analysis of abdominal aortic rings by wire myography showed a lower but not a significant decrease in phenylephrine-induced maximum contraction in *Nox4*TG605 (Fig. 2*B*) and a 57% decrease in *Nox4*TG618 (Fig. 2*C*; $P < 0.05$) mice versus wild-type mice. Consistent with this, dose response curve showed that the response to phenylephrine was similar between wild-type and *Nox4*TG605 mice (Fig. 2*D*), whereas *Nox4*TG618 mice showed impaired aortic contraction compared with the wild-type mice (Fig. 2*E*; $P < 0.05$). However, endothelium-dependent relaxation to acetylcholine after pre-contraction with phenylephrine (*SI Appendix*, Fig. S1 *A* and *B*) and endothelium-independent relaxation to sodium nitroprusside (Fig. S1 *C* and *D*) were not affected in young *Nox4*TG mice.

We performed collagen gel contraction assay to determine whether the decrease in maximum contractile force in response to phenylephrine is partly contributed by NOX4-induced changes in the contractile phenotype of aortic SMCs [31]. Gel contraction mediated by aortic VSMCs from wild-type and *Nox4*TG605 was similar (Fig. 2 *F* and *G*). In comparison, the reduction in gel contraction was significantly attenuated with aortic VSMCs isolated from *Nox4*TG618 mice (Fig. 2 *F* and *G*), indicating that increase in mitochondrial NOX4 expression levels induces VSMC stiffening.

Increase in Intrinsic Stiffness of Aortic VSMCs Contributes to Aortic Stiffening in Young Nox4 Transgenic Mice. To further explore the underlying mechanism for the reduction in gel contraction observed with *Nox4*TG618 VSMCs and also because aortic stiffness with aging is attributed to intrinsic changes in VSMCs [32], we determined single VSMC stiffness using atomic force microscopy. As shown in Fig. 3, elastic modulus, a measure of stiffness, was significantly higher in aortic VSMCs from young *Nox4*TG618 (21.0 ± 1.3 kPa, 10 cells, 150 measurements) compared with cells from young wild-type mice (13.0 ± 0.66 kPa, 10 cells, 105 measurements), further supporting the notion that mice with increased mitochondrial NOX4 expression phenocopy vascular aging.

Increase in Mitochondrial NOX4 Expression Induces Age-associated Extracellular Matrix Remodeling. Age-dependent increase in aortic wall stiffness is attributed to extracellular remodeling, including fibrosis [33] and we reported previously that treatment with mitochondria-targeted antioxidant, MitoTEMPO, significantly lowers aortic wall collagen content and pulse wave velocity (PWV) in mouse models of atherosclerosis [12]. Hence, we first determined expression of immunoreactive connective tissue growth factor (CTGF), an

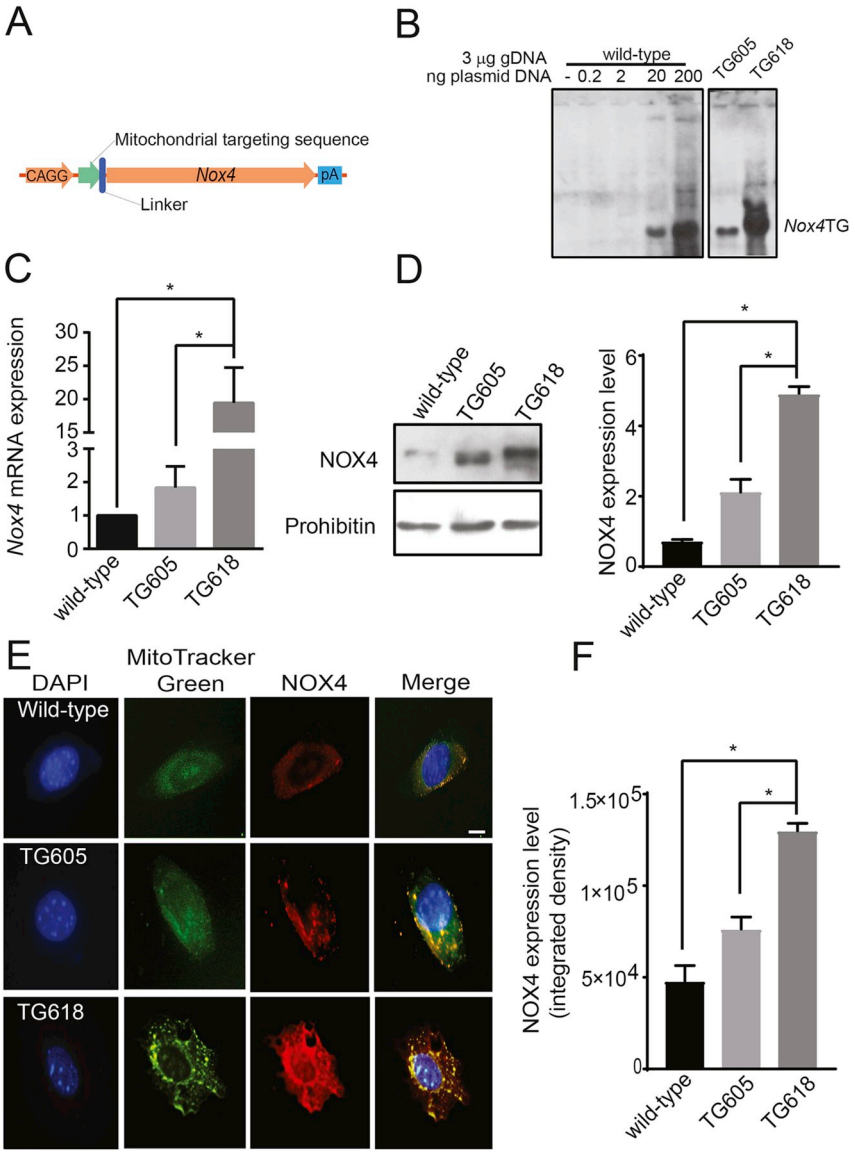

Fig. 1. Generation and characterization of mitochondrial-specific *Nox4* transgenic mice. (*A*) Essential features of the full length *Nox4* overexpressing construct are depicted in the cartoon. The *Nox4* gene is preceded by a Chicken β-actin promoter and a mitochondrial targeting sequence (*B*) Southern blot analysis for estimation of *Nox4* transgene copy number in *Nox4*TG605 (low expresser) and *Nox4*TG618 (high expresser). Relative *Nox4* gene copy number was assessed by spiking the wild-type genomic DNA with 0.2, 2, 20 or 200 ng of the transfection plasmid containing full length *Nox4* gene. (*C*) Real-time reverse transcription polymerase chain reaction analysis of *Nox4* mRNA expression in aortic VSMCs (mean ± SEM, $N = 6$). (*D*) Western blot analysis of NOX4 protein levels from liver mitochondria of the transgenic mice along with mitochondrial marker protein prohibitin (left panel). Densitometric quantification of NOX4 levels normalized to prohibitin levels (right panel; mean ± SEM, $N = 4$) (*E*). Representative confocal microscopy images of VSMCs showing NOX4 localization to mitochondria in wild-type, TG605, and TG618 mice. Cells were stained with MitoTracker Green FM and rabbit anti-NOX4 and AlexaFluor 647 rabbit anti-goat IgG. Bright yellow fluorescence indicates increased NOX4 levels in mitochondria. (*F*). Data presented was integrated density of NOX4 and MTG fluorescence (mean ± SEM, $N = 30$). Scale is 10 μm $^*P < 0.05$. (For interpretation of the references to colour in this figure legend, the reader is referred to the Web version of this article.)

important regulator of fibrosis [34], in aortic cross sections. CTGF expression was significantly higher in the aortas of young *Nox4*TG mice versus the wild-type and correlated with NOX4 levels (Fig. 4*A*). Congruently, aortic wall collagen content was higher in young *Nox4*TG mice versus the wild-type, with young *Nox4*TG618 mice showing a significant increase (Fig. 4*B*).

To determine the clinical relevance of relationship between NOX4 expression and aging-associated arterial fibrosis, we examined NOX4, CTGF, and collagen expression levels in the carotid artery cross sections of young and older human subjects. Corroborating the data from our mouse models, carotid artery wall NOX4, CTGF, and collagen levels were significantly higher in the older subjects compared with the young (Fig. 4*C-E*). Together, these and above data suggest that NOX4 contributes to age-associated increase in aortic stiffness by both remodeling the extracellular matrix as well as inducing intrinsic stiffness of VSMCs.

NOX4 Overexpression Induces Structural Changes Associated with Aging, Impacting Aortic Elasticity and Volume Compliance. Aortic stiffness is linearly correlated with subendothelial matrix elastic modulus [35]. Hence, we measured the mechanical modulus of abdominal aortas using pressure myography [36]. The aortic rings from abdominal aortas of young *Nox4*TG618 mice showed a progressive and significant left ward shift in stress-strain relationship compared with aortic rings from the wild-type mice, indicating increased aortic stiffness (Fig. 5*A*). However, aortic wall thickness and outer diameter were not different between the two genotypes (Fig. 5 *B* and *C*). A significant reduction in aortic volume compliance was observed in young *Nox4*TG618 mice at physiological pressures (110 and 130 mmHg) compared with the age-matched wild-type mice (Fig. 5*D*).

Focal adhesions, which connect the cortical cytoskeleton of VSMCs to the matrix in aortic wall, are an important regulator of aortic stiffness [37] and NOX4 is implicated in focal adhesion stability [38]. To determine whether focal adhesions play a role in aging-associated aortic stiffness, we compared focal adhesion number and turnover in aortic VMSCs of young wild-type and *Nox4*TG618 mice. As assessed by immunostaining for autophosphorylation of focal adhesion kinase (FAK) on tyrosine 397, which increases under conditions associated with enhanced focal adhesion formation [39], *Nox4*TG618 VSMCs had significantly higher number of focal adhesions compared with the wild-type VSMCs (Fig. 5*E*). In addition, nocodazole-induced microtubule-dependent focal adhesion turnover at 15 and 45 min following nocodazole washout was significantly lower in *Nox4*TG618 VSMCs. Further characterizing the structural changes in age-associated aortic stiffening, we measured the expression of load-bearing protein collagen I [40]. As shown in Fig. 5*F*, aortic collagen I levels were significantly increased in young *Nox4*TG618 mice, mainly as a result of greater expression in the adventitia. Hyaluronan expression is regulated by NADPH oxidases

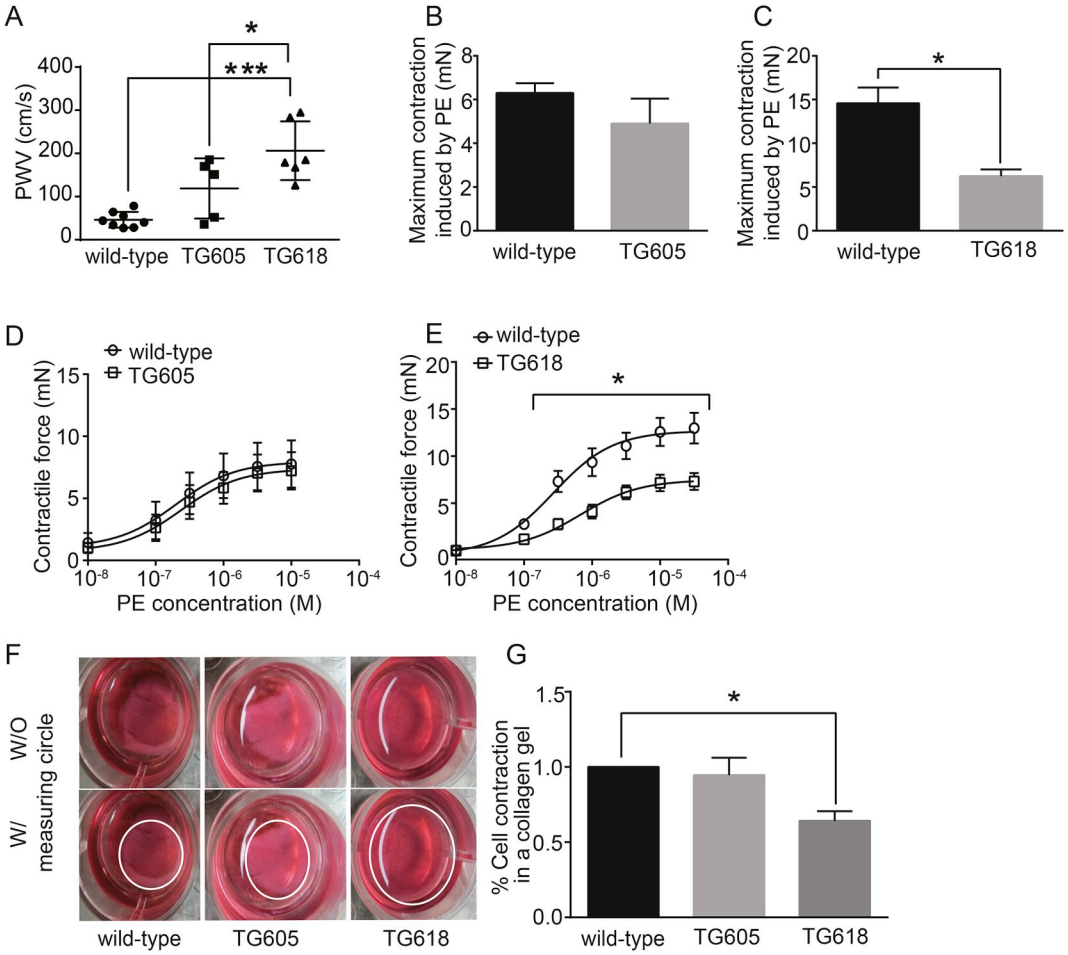

Fig. 2. Young (4-month old) *Nox4* transgenic mice with high mitochondrial NOX4 expression show increased aortic stiffness and reduced contractile function in aorta and VSMCs. (*A*) Pulse wave velocity (PWV) was measured in wild-type, *Nox4*TG605, and *Nox4*TG618 mice (mean ± SEM, $N = 5–8$; $^{*}P < 0.05$ versus *Nox4*TG605, $^{***}P < 0.001$ versus wild-type). Maximal contractile force in abdominal aortic rings in response to phenylephrine (PE, 3.16×10^{-5} M) was measured by wire myography in (*B*) wild-type and *Nox4*TG605 and (*C*) wild-type and *Nox4*TG618 mice (mean ± SEM, $N = 7$; $^{*}P < 0.05$). The force generation dose-response curves for PE were shown for (*D*) wild-type and *Nox4*TG605 and (*E*) wild-type and *Nox4*TG618 aortic rings (mean ± SEM, $N = 7$). (*F* and *G*) VSMC contraction was measured using collagen gel-based contraction assay kit and the area of the dislodged gel was measured using NIH image J software (mean ± SEM; n = 6; $^{*}P < 0.05$).

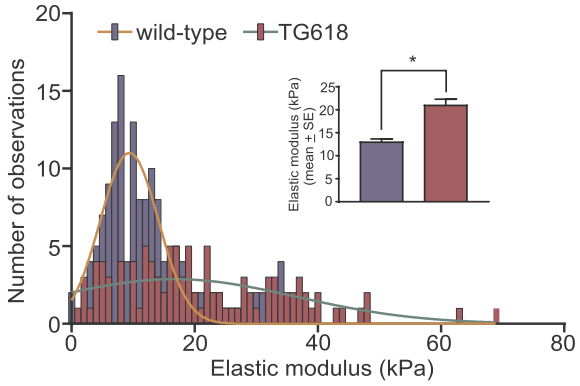

Fig. 3. Aortic VSMCs from *Nox4*TG618 mice show increased cellular stiffness. Histogram represents cellular stiffness (elastic modulus), measured by atomic force microscopy, derived from cantilever deflection data for at least 10 VSMCs per genotype (10 cells for each genotype; 150 observations for wild-type and 105 for TG618). The solid curves are a fit to a normal distribution. Inset shows the mean elastic modulus ± SEM. $^{*}P < 0.05$. The atomic force microscopy measurements were repeated with two more aortic VSMC isolates and with similar results.

[41] and aortic stiffening was attributed to increased hyaluronan accumulation [42]. Analysis of hyaluronan expression, as measured by immunoreactive hyaluronan binding protein levels, showed a marked increase in aortic hyaluronan levels in *Nox4*TG618 versus wild-type mice (Fig. 5*G*). Lastly, we examined aortic medial calcium deposition by von Kossa staining as calcification increases aortic stiffening [12]. As shown in Fig. 5*H*, aortic calcium deposition was significantly higher in young *Nox4*TG618 versus wild-type mice. Together, these data support the notion that increase in NOX4 levels, particularly in mitochondria, play a major role in vascular aging.

Young Nox4TG Mice Show Elevated Aortic and VMSC Mitochondrial H_2O_2 and Superoxide Production. To determine whether vascular aging and aortic stiffness observed in *Nox4*TG mice is mediated by increased oxidative stress, we first measured H_2O_2 production, using Amplex Red assay, in abdominal aortic segments and mitochondrial isolates from VSMCs. Aortic H_2O_2 levels increased 51 and 146% in *Nox4*TG605 and TG618 mice, respectively, compared with the wild-type mice (Fig. 6*A*). Similarly, a significant and transgene expression-dependent mitochondrial H_2O_2 production was observed in VSMCs, with 37 and 76% increase in *Nox4*TG605 and TG618 mice, respectively, compared with the wild-type mice (Fig. 6*B*).

Although NOX4 predominantly produces H_2O_2[9], NOX4 expression is also correlated with increased superoxide levels [16]. In line

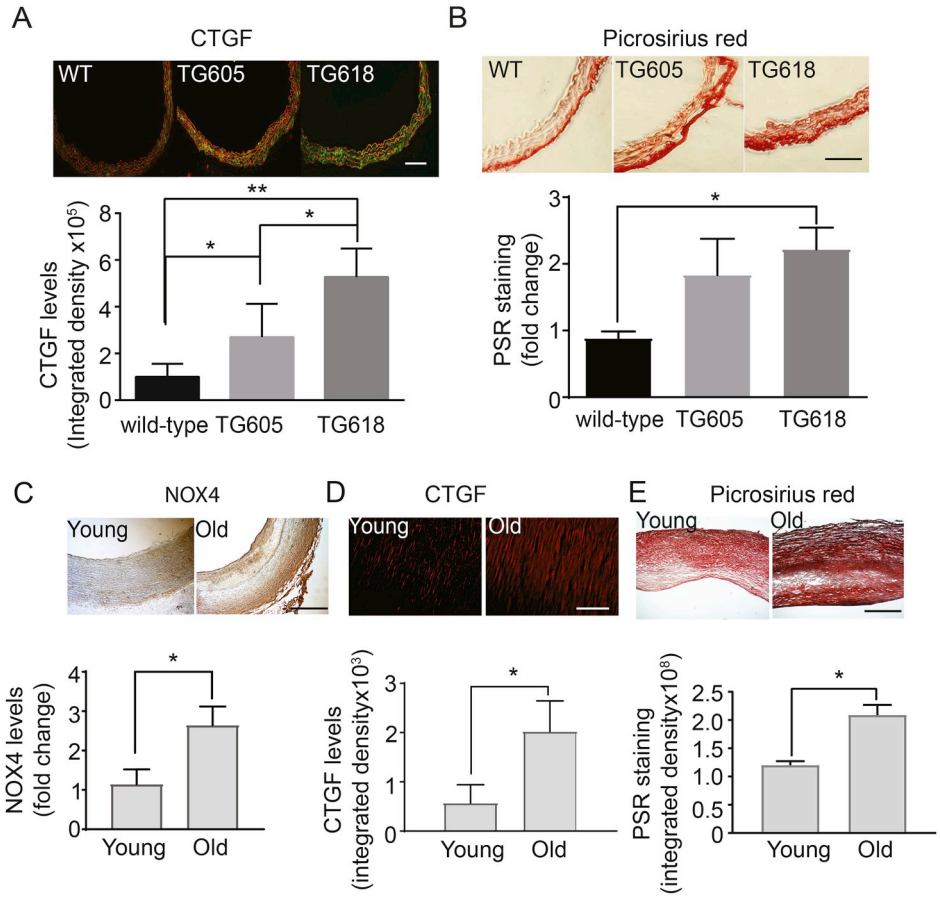

Fig. 4. Increase in NOX4 expression is associated with vascular fibrosis in young Nox4TG mice and older human subjects. Representative images of mouse aortic sections stained for immunoreactive connective tissue growth factor (*A*, CTGF, green, red = elastin autofluorescence, scale 100 μm) and stained with picrosirius red (*B*, scale 100 μm). CTGF levels (*A*, bottom panel) and picrosirius red staining (*B*, bottom panel) presented as integrated density (mean ± SEM, $N = 5–10$). Representative carotid artery sections from young and old subjects stained for immunoreactive NOX4 (*C*, *brown*, scale 500 μm) and CTGF (*D*, *red*, scale 500 μm) and stained with picrosirius red (*E*, scale 500 μm). NOX4 (C, bottom panel) and CTGF levels (*D*, bottom panel) and picrosirius red staining (E, bottom panel) presented as integrated density (mean ± SEM, $N = 5–10$). $^{*}P < 0.05$, $^{**}P < 0.01$ and $^{***}P < 0.001$. (For interpretation of the references to colour in this figure legend, the reader is referred to the Web version of this article.)

with this, transgene expression-dependent increase in mitochondrial superoxide levels, as measured by MitoSOX Red fluorescence, was observed in medial VSMCs in aortic cross sections of young *Nox4*TG mice compared with the wild-type mice (Fig. 6*C*). Cellular superoxide levels, as determined by DHE fluorescence, increased significantly in medial VSMCs of *Nox4*TG618 compared with the *Nox4*TG605 and wild-type mice (Fig. 6*C*). Similarly, transgene expression-dependent increase in mitochondrial and cellular superoxide levels was observed in VSMCs from *Nox4*TG mice compared with the wild-type mice (Fig. 6*D*). Rotenone + antimycin A treatment markedly inhibited superoxide levels in VSMCs from *Nox4*TG618 mice, suggesting that increased superoxide levels were partly of mitochondrial origin (*SI Appendix*, Fig. S2). Inhibition of superoxide levels in the presence of MitoTEMPO and PEG-SOD in *Nox4*TG618 mouse aortic VSMCs further supports both mitochondria-derived and *Nox4* transgene-dependent increase in mitochondrial superoxide levels (SI Appendix, Fig. S2). Together, these data demonstrate that vascular oxidative stress was greater in aortas of *Nox4*TG618 mice with higher *Nox4* transgene expression.

Aortic VSMCs from Young Nox4TG Mice Show Increased DNA Damage and Apoptosis. Multiple levels of evidence have established a correlation between oxidative DNA damage and aging [12,14,43] and increased mitochondrial oxidative stress drives aging-induced vascular dysfunction via induction of apoptosis [44]. Hence, we investigated whether increased mitochondrial NOX4 expression in young *Nox4*TG mice induced oxidative DNA damage in aortic VSMCs. A 3.7-fold increase in VSMCs with comet tails was observed in *Nox4*TG618 mice compared with the wild-type mice (Fig. 7*A*). Although the number of VSMCs with comet tails also increased in *Nox4*TG605 mice, the increase was not significant compared with the wild-type mice. Congruent with this, long PCR amplification of 10 kb mitochondrial DNA was 2.3-fold lower in VSMCs of *Nox4*TG618 mice compared with *Nox4*TG605 and wild-type mice, indicating an increase in DNA lesions that are blocking mitochondrial DNA replication (Fig. 7*B*).

Furthermore, the expression of phosphorylated histone variant 2AX (γH2AX), which accumulates at DNA double-strand breaks and recruits DNA repair machinery [45], increased markedly in VSMCs from young *Nox4*TG618 mouse compared with *Nox4*TG605 and wild-type mice (Fig. 7*C*). In contrast, expression of the oxidative DNA base excision repair enzyme, 8oxoG DNA glycosylase [46] (OGG1) was significantly decreased in VSMCs from young *Nox4*TG618 mouse compared with *Nox4*TG605 and wild-type mice (Fig. 7*C*). Similarly, the expression of TFAM (transcription factor A, mitochondrial), which maintains mitochondrial DNA stability by binding it to form nucleoids and stimulating its replication [47] was greatly reduced in young *Nox4*TG618 mouse aortic VSMCs versus young wild-type mouse VSMCs (Fig. 7*C*). In addition, expression of superoxide dismutase 2 (SOD2), the principal scavenger of mitochondrial superoxide, was almost completely suppressed in young *Nox4*TG618 mouse VSMCs (Fig. 7*C*). Interestingly, TFAM and SOD2 expression were markedly upregulated in young *Nox4*TG605 mouse VSMCs versus the wild-type cells, suggesting that a moderate increase in NOX4 levels and hence, H_2O_2 levels over a relatively short duration induce mitochondrial transcription factor and antioxidant enzyme expression.

Next, we examined apoptosis in aortic sections by TUNEL-staining. As shown in Fig. 7*D*, a significant transgene expression-dependent increase in TUNEL^{+} medial SMC was observed in young *Nox4*TG605 and *Nox4*TG618 mice versus wild-type mice. In consonance with this data, a significant transgene expression-dependent increase in apoptosis was observed in *Nox4*TG618 and TG605 VSMCs versus wild-type VSMCs in culture (Fig. 7*E*). We also examined the expression of poly (ADP-ribose) polymerase (PARP), a DNA-binding protein, which is a determinant of cell viability in response to DNA damage [48], in aortic VSMCs with and without *Nox4* overexpression. As observed with TFAM and SOD2, VSMCs from young *Nox4*TG605 mice had a marked increase in PARP

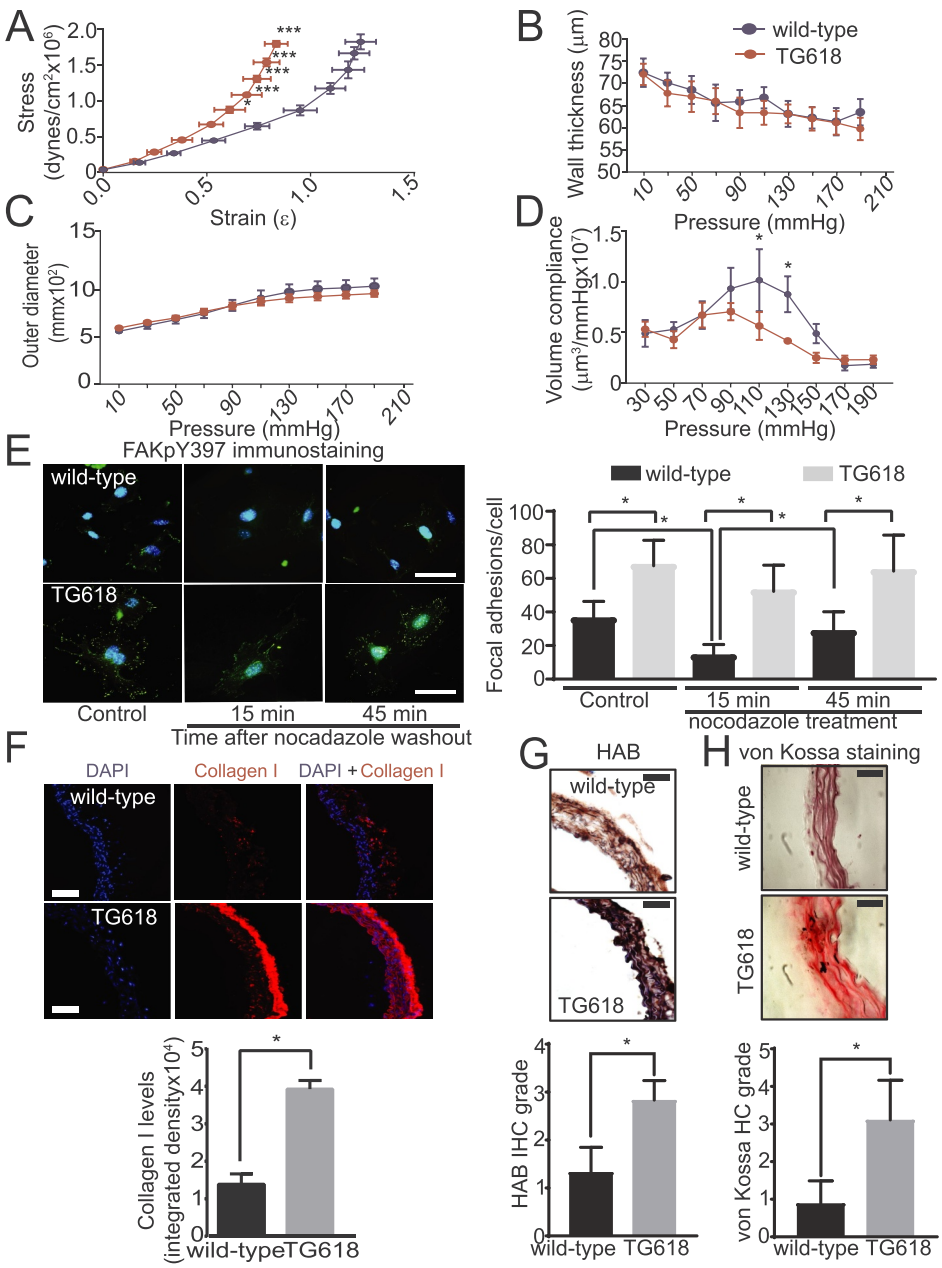

Fig. 5. Young *Nox4*TG618 mice show reduced aortic elasticity and volume compliance and structural changes associated with aging. Aortic elasticity (*A*), wall thickness (*B*), outer diameter (*C*), and volume compliance (*D*) were measured in wild-type and *Nox4*TG618 mice using pressure myograph (mean ± SEM, $N = 4$). (*E*) Representative images of VSMCs immunostained for phosphorylated focal adhesion kinase with FAKpY397 antibody (*green*) and counterstained with DAPI (*blue*) in the presence and absence of 10 μM nocodazole (left panel). Inhibition of focal adhesion turnover with increased NOX4 expression was quantified by FAKpY397 staining (mean ± SEM, $N = 25$; right panel). The experiment was repeated twice with similar results. (*F*) Representative immunofluorescence images of aortic cross sections stained for type I collagen (*red*, collagen I and *blue,* DAPI). Quantification of collagen I expression shown as fluorescence integrated density (mean ± SEM, $N = 6$). (*G*) Representative immunohistochemistry (IHC) sections stained for hyaluronan binding protein (HAB; top panel). Quantification of HAB expression shown as IHC grade (mean ± SEM, $N = 6$; lower panel). (*H*) Representative histochemistry (HC) sections stained with von Kossa stain (top panel). Quantification of calcium shown as HC grade (mean ± SEM, $N = 6$; lower panel). (For interpretation of the references to colour in this figure legend, the reader is referred to the Web version of this article.)

expression versus wild-type cells, whereas PARP expression was undetectable in *Nox4*TG618 VSMCs in Western blots (Fig. 7*F*). The fact that apoptosis is increased in *Nox4*TG605 versus wild-type cells suggests that more than one mechanism for inducing apoptosis is active in these cells.

Young Nox4TG Mice Show Increased Aortic VSMC Senescence and Proinflammatory Gene Expression. DNA damage accrual impairs tissue function and increases susceptibility to age-associated diseases by inducing replicative senescence [43]. Also, induction of premature senescence was reported in a number of cell types in response to oxidative stress [49] and NOX4 activity is correlated with replicative senescence in human umbilical vein endothelial cells [50]. Premature senescence, assessed by staining for senescence-associated β-galactosidase (SA-β-Gal) activity, increased significantly in young *Nox4*TG618 mice VSMCs compared with *Nox4*TG605 and wild-type mouse cells (Fig. 8*A*). In addition, cell proliferation as assessed by BrdU incorporation was 233% lower in VSMCs from young *Nox4*TG618 mice compared with the wild-type mice (Fig. 8*B*), indicating replicative senescence. The proliferation of *Nox4*TG605 VSMCs was not significantly different from wild-type cells.

In addition, VSMCs from young *Nox4*TG618 mice showed significantly increased Ser 317 phosphorylation of CHK1 and decreased Thr187 phosphorylation of $p27^{Kip1}$, supporting replication arrest with increased NOX4 expression (Fig. 8*C*) [51,52]. Inflammation is correlated with arterial stiffness [53] and we have shown that NOX4 regulates vascular inflammation in aging [15]. As shown in Fig. 8 *D* and *E*, the expression of transforming growth factor β1 (TGFβ1), a profibrotic cytokine, was 1.88-fold higher ($P < 0.05$) in VSMCs from young *Nox4*TG618 mice compared with the wild-type mice; *Nox4*TG605 mice VSMCs also show higher TGFβ1 levels, but the difference was not significant from the wild-type. Vascular cell adhesion molecule 1 (VCAM1) is among the genes identified in polymorphism association studies with a possible causal role in arterial stiffness [54]. In agreement with our previous observations [12,15], VSMCs from young *Nox4*TG618 mice with higher mitochondrial NOX4 levels had an approx. 56% increase ($P < 0.05$) in VCAM1 expression compared with VSMCs from wild-type and *Nox4*TG605 mice (Fig. 8 *D* and *F*). Together, these data suggest that increased mitochondrial oxidative stress and DNA damage in

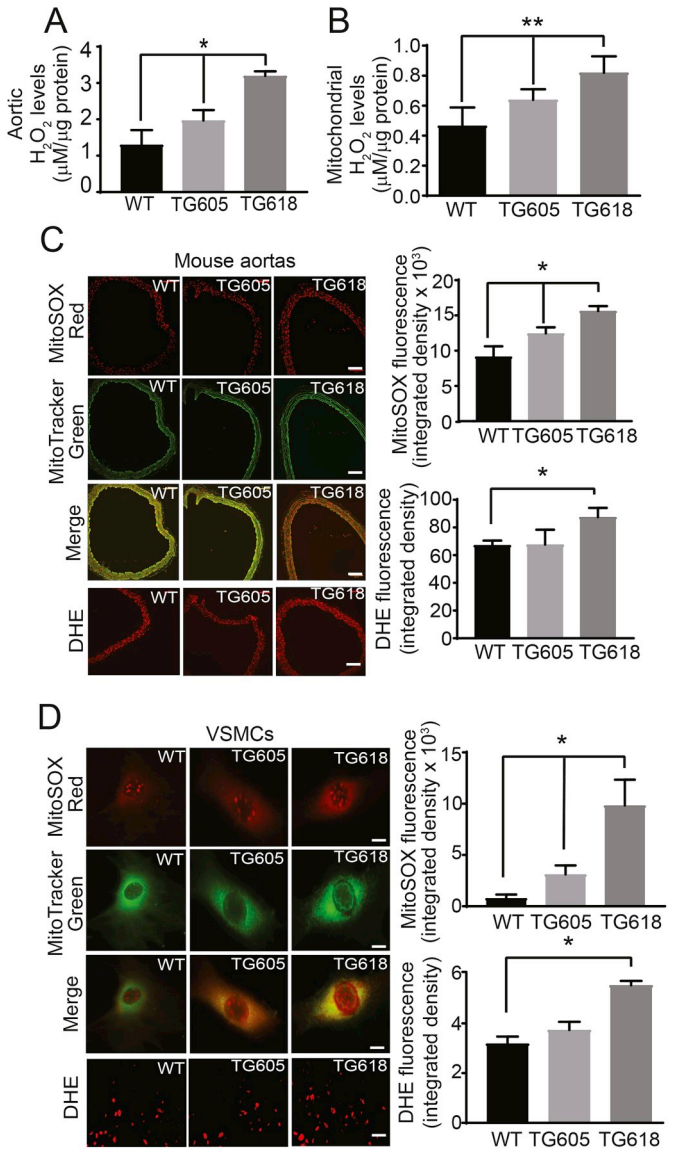

Fig. 6. Increase in mitochondrial NOX4 protein levels is correlated with enhanced H_2O_2 and ROS levels in whole aortas and aortic VSMCs. (*A*) Aortic H_2O_2 levels were determined using Amplex Red assay and normalized to protein levels (mean ± SEM, $N = 5$). (*B*) VSMC mitochondrial H_2O_2 levels were determined using Amplex Red assay. H_2O_2 levels are normalized to protein concentration and are the mean ± SEM of three independent experiments. (*C*) Representative fluorescence microscopy images of aortic sections stained with MitoSOX Red and MitoTracker Green FM. Bright yellow/orange fluorescence indicates increased mitochondrial ROS generation in medial VSMCs. Scale is 100 μm. Data presented as integrated density of MitoSOX Red fluorescence (mean ± SEM, $N = 5$). Representative DHE fluorescence microscopy images and quantification of DHE fluorescence in medial VSMCs (mean ± SEM, $N = 5$). Scale is 100 μm. (*D*) Representative fluorescence microscopy images of VSMCs stained MitoSOX Red and MitoTracker Green FM. Bright yellow fluorescence indicates increased ROS generation. Data presented was integrated density of MitoSOX Red fluorescence (mean ± SEM, $N = 30$). Scale is 10 μm. Representative DHE fluorescence microscopy images and quantification of DHE fluorescence in VSMCs (mean ± SEM, $N = 30$). Scale is 10 μm $^*P < 0.05$ and $^{**}P < 0.01$. (For interpretation of the references to colour in this figure legend, the reader is referred to the Web version of this article.)

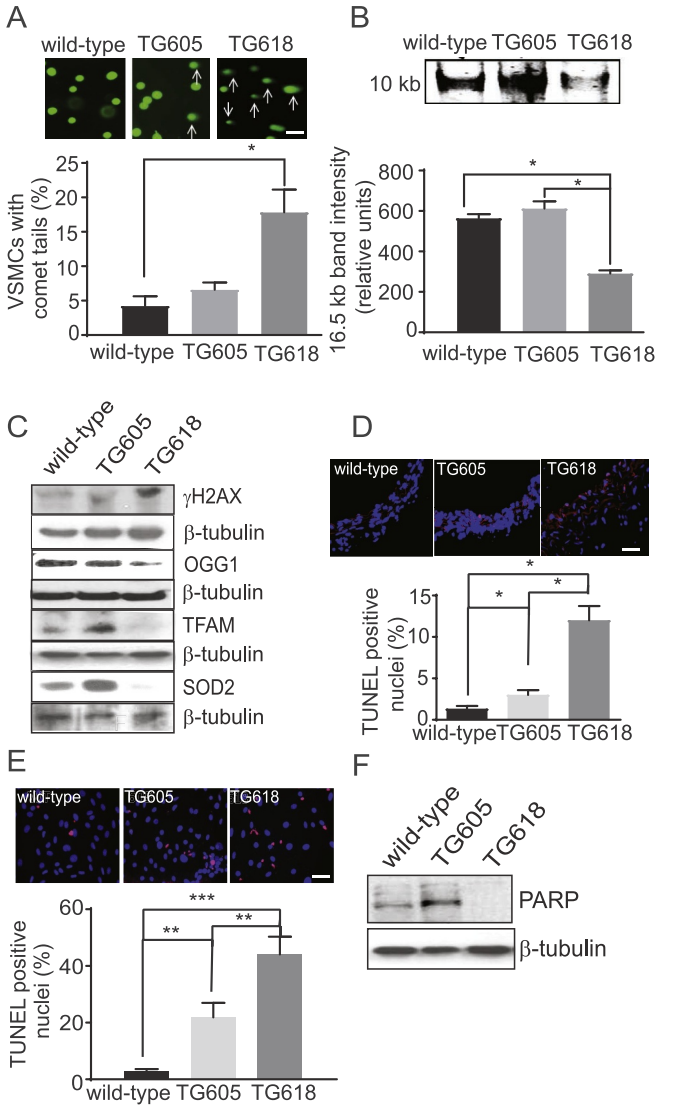

Fig. 7. Young *Nox4*TG mice show increased DNA damage and apoptosis in VSMCs. (*A*) Representative comet assay images and quantification of cells with comet tails in aortic VSMCs isolated from wild-type and *Nox4*TG mice. Percent of cells with comets from 15 microscopic areas from three independent experiments (mean ± SEM, $N = 3$). (*B*) Representative long PCR amplicon showing decreased 10 kb mitochondrial DNA in VSMCs from wild-type, *Nox4*TG605, and *Nox4*TG618 mice. The amplified 16.5 kb mitochondrial genome band intensity was normalized to a short PCR amplicon of 0.22 kb GAPDH (mean ± SEM, $N = 3$). (*C*) Representative Western blots of VSMC lysates indicate more DNA damage and increased oxidative stress, as shown by increased levels of γH2AX and decreased levels of OGG1, TFAM, and SOD2 in *Nox4*TG618 versus *Nox4*TG605 and wild-type mice. (*D*) Representative fluorescent microscopy images of TUNEL-stained aortic sections showing increased TUNEL$^+$ nuclei in medial VSMCs of *Nox4*TG618 versus *Nox4*TG605 and wild-type mice. Quantification of TUNEL$^+$ nuclei (mean ± SEM, $N = 3$). (*E*) Representative fluorescent microscopy images of TUNEL-stained VSMCs showing increased TUNEL$^+$ nuclei in *Nox4*TG618 versus *Nox4*TG605 and wild-type VSMCs. Quantification of TUNEL$^+$ nuclei (mean ± SEM, $N = 3$). (*F*) Western blot analysis of PARP expression levels in aortic VSMCs of wild-type and *Nox4*TG mice. Data shown are representative of three independent experiments. $^*P < 0.05$, $^{**}P < 0.01$ and $^{***}P < 0.001$.

young *Nox4*TG618 mice phenocopy premature and replicative senescence and increased vascular inflammation associated with aging which contributes to aortic stiffening.

Increased NOX4 Expression Induces Mitochondrial Dysfunction in Young *Nox4*TG Mice. We previously showed that increased expression/activity of mitochondrial NOX4 in aging was correlated with decreased vascular respiratory chain complex activity and bioenergetics [12]. Also, impaired mitochondrial respiration is a key factor in organismal functional decline and may result from and contribute to

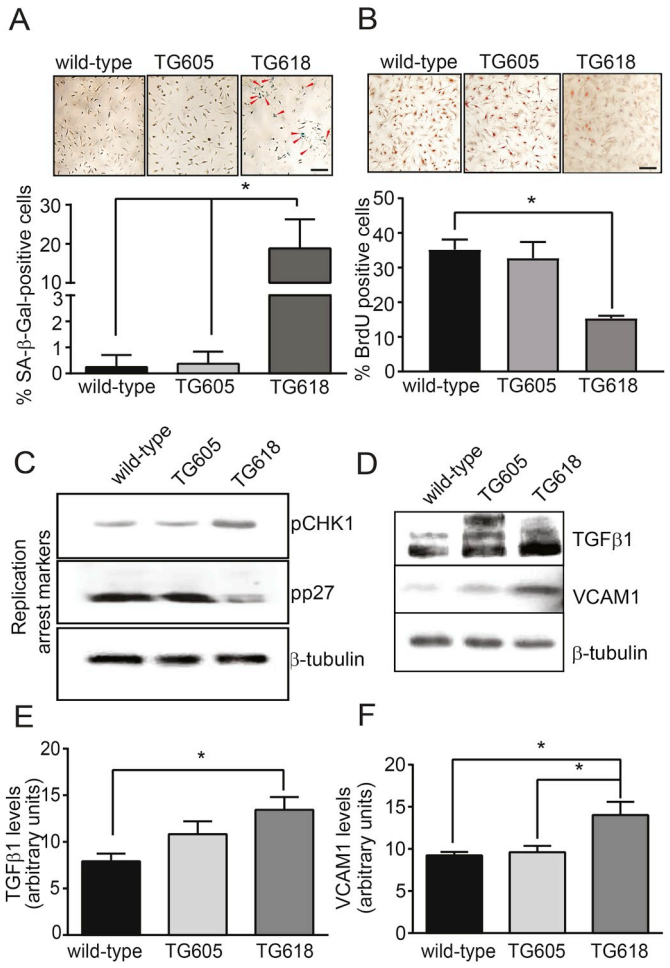

Fig. 8. Increase in mitochondrial NOX4 protein level induces senescence and pro-inflammatory marker expression in VSMCs. (*A*) Representative brightfield microscope images of VSMCs stained for SA-β-Gal activity (upper panel) and % SA-β-Gal-positive cells (lower panel, mean ± SEM, $N = 3$). (*B*). VSMC proliferation rate was determined by BrdU incorporation (representative brightfield microscope images, upper panel) and the number of BrdU-positive cells (lower panel) was assessed as described in Methods section (mean ± SEM, $N = 3$). Scale is 10 μm in *A* and *B*. (*C*) Representative Western blots showing protein levels of replication arrest markers pCHK1 (phospho checkpoint kinase 1, Ser^{317}) and pp27 (phospho KIP1, Thr^{187}) in 60% confluent VSMCs. (*D*) Representative Western blots showing protein levels of proinflammatory makers TGFβ1 and VCAM1. β-tubulin was used as a loading control in *C* and *D*. Densitometric quantification of TGFβ1 (*E*) and VCAM1 protein levels normalized to β-tubulin levels (*F*). $^*P < 0.05$.

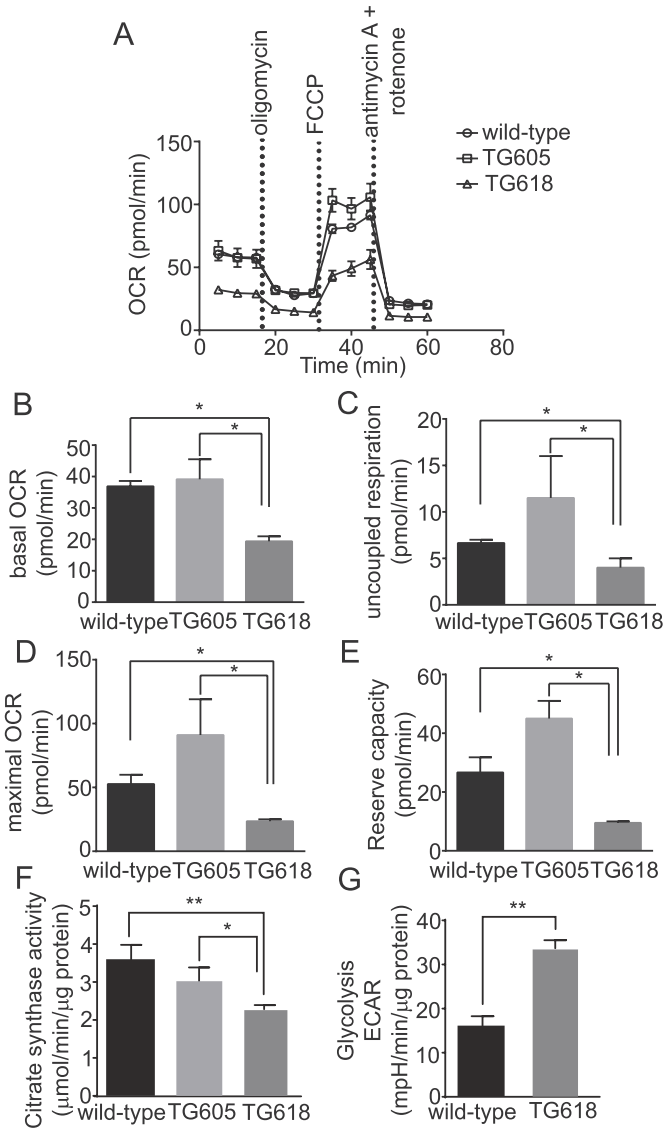

Fig. 9. Young *Nox4* transgenic mice with high mitochondrial NOX4 expression show reduced respiration in aortic VSMCs. (*A*) Oxygen consumption rate (OCR) of aortic VSMCs isolated from wild-type, *Nox4*TG605, and *Nox4*TG618 mice was determined using Seahorse XF-24 analyzer. VSMCs were plated at 25,000 cells/well in XF-24 plates and OCR was measured at the basal levels and in the presence of 2 μM oligomycin, 500 nM trifluoromethoxy carbonylcyanide phenylhydrazone (FCCP), and 0.5 μM antimycin A + 500 nM rotenone. Data shown are mean ± SEM, $N = 3$. Mitochondrial bioenergetic parameters derived from OCR measurements are: (*B*) basal OCR, (*C*) uncoupled OCR, (*D*) maximal OCR, and (*E*) respiratory reserve capacity (mean ± SEM, $N = 3$). *(F)* VSMC citrate synthase activity levels (mean ± SEM, $N = 3$). *(G)* Extracellular acidification rate (ECAR) of aortic VSMCs from the wild-type and *Nox4*TG618 mice was determined using Seahorse XFp analyzer. VSMCs were plated at 30,000 cells/well in XFp plates and ECAR was measured at the basal level (no glucose) and in the presence of 10 mM glucose and 1 μM oligomycin and the data were normalized to protein concentration (mean ± SEM, $N = 3$). $^*P < 0.05$, $^{**}P < 0.01$, $^{***}P < 0.001$, $^{****}P < 0.0001$.

increased H_2O_2 production [55]. VSMCs from young *Nox4*TG18 showed a significant decrease in basal, ATP-driven, and maximal mitochondrial oxygen consumption rate (OCR; $P < 0.05$) compared with VSMCs from young wild-type and *Nox4*TG605 mice (Fig. 9 *A-D*). Bioenergetic analysis also showed significant decreases in mitochondrial reserve respiratory capacity, uncoupled OCR and non-mitochondrial respiration in *Nox4*TG18 VSMCs versus wild-type and *Nox4*TG605 VSMCs (Fig. 9 *A-E*). All the bioenergetic parameters analyzed were higher in *Nox4*TG605 VSMCs versus wild-type cells, but the differences were not significant. Correlating with decreased OCR data, citrate synthase activities in *Nox4*TG618 VSMCs were significantly lower compared with the *Nox4*TG605 and wild-type VSMCs (Fig. 9 *F*). Compensating the diminished mitochondrial oxidative capacity, glycolysis increased significantly in *Nox4*TG18 VSMCs versus the wild-type cells ($P < 0.01$; Fig. 9 *G*). These data support a role for increased mitochondrial NOX4 levels in aging-associated mitochondrial dysfunction.

Young *Nox4*TG618 and m*CAT* Double Transgenic Show Attenuated Aortic Stiffness. Rabinovitch and colleagues showed that overexpression of human catalase in mitochondria attenuated ventricular fibrosis and hypertrophy associated with myocardial stiffness in old mice [56]. Similarly, attenuation of mitochondrial oxidative stress by supplementation with MitoQ, a mitochondria-targeted antioxidant, ameliorated aortic stiffening in old mice [57] and older adults [58]. The loss of SOD2 expression increases the initial mitochondrial superoxide levels in *Nox4*TG618 aortic medial VSMCs. The mitochondrial

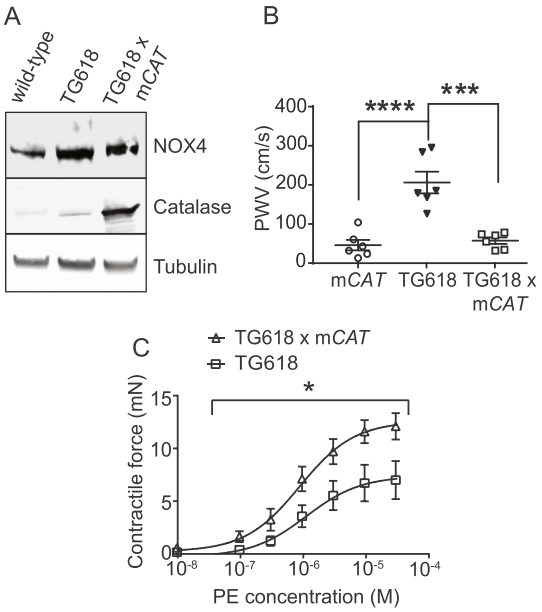

Fig. 10. Overexpression of catalase targeted to mitochondria attenuates aortic stiffness and contractile function in young *Nox4*TG mice. (*A*) Western blot analysis of NOX4 and catalase expression in aortic lysates. (*B*) PWV was measured in m*CAT* (transgenic mice with overexpression of human catalase in mitochondria), *Nox4*TG618, and *Nox4*TG618 x m*CAT* mice (mean ± SEM, $N = 6$; ***$P < 0.001$, ****$P < 0.0001$; One-way ANOVA with Tukey's multiple comparison test). (*C*) The force generation dose-response curves for PE were shown for *Nox4*TG618 and *mCAT x Nox4*TG618 *aortic* rings (mean ± SEM, $N = 7$; *$P < 0.05$).

superoxide levels are further increased by mitochondrial NOX4-derived superoxide [16]. However, superoxide spontaneously dismutates to H_2O_2 quite rapidly in concentration-dependent manner. To confirm that vascular aging in young *Nox4*TG618 is mediated by increased mitochondrial oxidative stress, we measured PWV in young *Nox4*TG618 mice with (*Nox4*TG618 x m*CAT* mice) *and* without overexpression of mitochondria-targeted human catalase. Fig. 10*A* shows overexpression of NOX4 and catalase in young *Nox4*TG618 x m*CAT* double transgenic mice. PWV was significantly attenuated in young double transgenic mice compared with young *Nox4*TG618 (Fig. 10*B*; $P < 0.001$). Furthermore, comparison of dose response curves showed that overexpression of catalase in mitochondria reversed the decreased phenylephrine-induced contractile force generation in *Nox4*TG618 mice (Fig. 10*C*), thus confirming the role of mitochondrial NOX4 in aging-associated impaired vasomotor function. Together, our present and previous studies [12,22] show that mitochondrial oxidative stress is a causal factor in aortic stiffness and vascular aging.

2. Discussion

This study presents evidence that increase in mitochondrial ROS, from increased NOX4 expression/activity in mitochondria, is a causative factor in aging-associated aortic stiffening as young *Nox4*TG618 mice with mitochondrial targeted NOX4 overexpression phenocopy aortic stiffening in aging. We confirmed increased *Nox4* expression in the transgenic mice by Southern blot and mRNA expression analyses, increased NOX4 protein by Western blot analysis, and increased mitochondrial NOX4 levels by confocal immunofluorescence. Our results also show that mitochondrial ROS levels beyond the physiological threshold level are necessary for aortic stiffening because young *Nox4*TG605 mice with a twofold increase in mitochondrial ROS levels do not show increased aortic stiffening.

The effect of higher NOX4 expression at the cellular level in vasculature was evident by increased VSMC mitochondrial and aortic H_2O_2 levels and enhanced cellular and mitochondrial superoxide levels in isolated aortic VSMCs and in medial VSMCs in aortic cross sections, establishing the role of increased NOX4-derived ROS in recapitulating aging-associated aortic stiffening in young *Nox4*TG618 mice. That mitochondrial oxidative stress is a key factor in age-associated aortic stiffening is supported by our previous studies [12,22] and other studies [23,57] in animal models. The potential clinical relevance of mitochondrial oxidative stress in age-associated aortic stiffness is evident in a randomized, placebo-controlled, double-blind, crossover design pilot study by Seals and colleagues [58] which showed that chronic supplementation with MitoQ significantly improved endothelium-dependent brachial artery flow-mediated dilation and lowered aortic stiffness and oxidized LDL levels in older adults.

Consistent with the data from classical studies of vascular mechanics that extracellular matrix is the major contributor to vessel wall stiffness [59,60], increased mitochondrial oxidative stress in young *Nox4*TG618 mice increased aortic stiffness as shown by stress-strain curves; congruently, volume compliance was reduced. In addition, increased mitochondrial ROS impaired phenylephrine-mediated aortic contraction in young *Nox4*TG618 mice and collagen gel contraction assay showed that decreased aortic contraction is mostly mediated by mitochondrial oxidative stress-induced changes in the contractile phenotype of aortic SMCs, although decrease in overall medial cellularity could contribute to impaired aortic contraction as well since *Nox4*TG618 aortic cross sections show increase in TUNEL$^+$ SMCs. It is interesting that increased mitochondrial NOX4 expression, while impairing aortic SMC contraction, has no effect on both endothelium-dependent and independent vasorelaxation.

Our data show that young *Nox4*TG618 mice with increased aortic stiffening had increased aortic collagen I expression, which renders extracellular matrix more rigid [61]. Collagen I expression, higher in the aortic media of transgenic mice, was more predominant in the adventitia and might reflect the transdifferentiation of adventitial fibroblasts to collagen synthesizing myofibroblasts in conditions of increased mitochondrial stress as happens in aging. This is in agreement with a previous report that arterial stiffening in aging is mediated by increased adventitial collagen I induced by increased levels of TGFβ1 [62], a NOX4 inducer [15].

Another contributing factor in the recapitulation of aging-associated aortic stiffness in young *Nox4*TG618 mice is increased number of focal adhesions and impaired focal adhesion turnover. Our data show markedly increased number of focal adhesions as observed by increased tyrosine 397 autophosphorylation and activation of focal adhesion kinase (FAK) in *Nox4*TG618 aortic VSMCs [61]. The activated FAK is bound by the SH2 domain of Src kinase and the activated FAK-Src complex allows the phosphorylation of other focal adhesion proteins [63]. Nocodazole removal induces microtubule repolymerization in 5–15 min and maximal dissolution of focal adhesions at 30 min [38]. The *Nox4*TG618 VSMC focal adhesions are resistant to nocodazole induced dissolution, which is in line with a previous report that persistent FAK-Src signaling complex of focal adhesions in non-migratory and quiescent VSMCs in the vessel wall is a significant regulator of aortic stiffness [37]. Normal aortic VSMC focal adhesions with an inherent ability to regulate their maturation and connections to nonmuscle cytoskeleton accommodate changes in vessel stress and stiffness in young mice [60]. In contrast, impaired VSMC focal adhesion dynamics with dissolution resistant adhesions under increased mitochondrial oxidative stress conditions compromise the ability of aorta and other large elastic vessels to maintain vessel tone in response to changes in hemodynamics. It is worth noting in this context that NOX4 localizes to and H_2O_2 is produced in focal adhesions and is required for focal adhesion stabilization, albeit in migrating VSMCs [38]. Also, the activity of small GTPase RhoA, which is upstream of FAK activation in focal adhesion formation, is activated by ROS produced by NOX4[38].

Young *Nox4*TG618 mice show increased nuclear and mitochondrial DNA damage and premature and replicative senescence in aortic

VSMCs, which is in line with evidence that accrual of DNA damage triggers cellular senescence and metabolic changes that impair tissue function and increase susceptibility to age-related diseases [43]. In addition, VSMCs from these mice show decreased OGG1 levels, indicating impaired DNA repair capacity and TFAM levels, indicating reduced mitochondrial biogenesis. Decreased TFAM levels could increase ROS levels in a feed forward manner and induce senescence since mitochondrial dysfunction caused by TFAM inactivation increased ROS levels and induced cell cycle arrest, ultimately resulting in lethal cardiomyopathy [64]. Although counterintuitive, another feed forward mechanism for increased ROS levels with significantly higher mitochondrial NOX4 levels in young *Nox4*TG618 mouse aortic VSMCs could be the suppression of SOD2 expression. Ji et al. reported that miR-146a, a widely expressed microRNA that is upregulated by H_2O_2, interacts with *Sod2* regulatory region and downregulates SOD2 protein expression via a post-transcriptional regulation mechanism [65].

Several clinical studies have shown significantly higher aortic stiffness in patients with several chronic inflammatory disorders and its association with increasing tertiles of different inflammatory biomarkers, including leukocyte and granulocyte count [66]. Increased VCAM1 expression in young *Nox4*TG618 mouse aortic VSMCs might enable extravasation of circulating leukocytes into the aortic wall, increasing aortic stiffness. Interestingly, aortic stiffening was associated with inflammation mediated adventitial collagen deposition by T cells [67] and cytomegalovirus-specific senescent $CD8^+$ T cells [68].

Our data showing attenuated aortic stiffness and improved aortic contractility in young *Nox4*TG618 mice with mitochondrial-targeted overexpression of catalase confirms the role of mitochondrial oxidative stress in aging-associated aortic stiffness as reported previously by us [12,22] and others [23,57,58]. Analogous amelioration of mitochondrial oxidative stress using mitochondrial antioxidant MitoTEMPO significantly reduced aortic stiffness in aged hypercholesterolemic mice [12]. Similarly, trehalose which enhances mitophagy and reduces ROS levels and MitoQ reduced aortic stiffness in old mice but had no effect in young mice [23]. Remarkably, oral supplementation with MitoQ for a short period of 6 weeks significantly lowered aortic stiffness in older adults in a pilot study [58], indicating the therapeutic potential of targeting mitochondrial oxidative stress for the treatment of large artery stiffness.

In summary, our results provide evidence that increased mitochondrial NOX4 levels have a causative effect on vascular aging by inducing intrinsic VSMC stiffness, extracellular matrix remodeling, aortic calcification and VSMC senescence, apoptosis, and inflammation by increasing mitochondrial oxidative stress. Because aortic stiffness is associated with several cardiovascular risk factors such as smoking, diabetes mellitus, dyslipidemia, and hypertension and is a major contributor to cardiovascular events, preventing and treatment of aortic stiffness by preserving mitochondrial homeostasis, either via targeting NOX4 expression/activity or using mitochondrial antioxidants, may be a viable new therapeutic option for age-related CVD.

3. Materials and Methods

Mice. All procedures were performed in compliance with protocols approved by the University of Michigan Institutional Animal Care and Use Committee in accordance with NIH guidelines. To generate NOX4 transgenic mice, the transgene DNA consisting of the CAG promoter (chicken beta-actin promoter with cytomegalovirus early enhancer) driving the mouse *Nox4* expression cassette preceded by a mitochondria targeted sequence of human cytochrome C oxidase was injected into pronuclei of C57BL/6 embryos and implanted into pseudo-pregnant foster female mice. The resulting offspring were analyzed for the insertion of the transgene construct and the founder lines with single transgene integration were identified by Southern blot analysis. The mouse genomic DNA was digested with BsrG1 and hybridized with a probe to the CMV enhancer of the transgene. A standard curve was developed using increasing concentrations of *Nox4* transgene plasmid DNA (0.2, 2, 20 and 200 ng). The founders were crossed with wild-type C57BL/6J mice to establish independent breeding lines. University of North Carolina Animal Models Core Facility performed transgene cloning, embryo microinjection and founder Southern blot analysis. The *Nox4* transgene-positive offspring were identified by PCR using following primers: 5'-TTCGGCTTCTGGCGTGTGAC-3' and 5'-CAACATTT GGTGAATGTAGTAGTATTCTGGC-3'. All breeder lines were backcrossed with C57BL/6J mice for 10 generations and lines with low (TG605) and high (TG618) *Nox4* expression levels were identified by qPCR and Western blot analysis. TG618 were crossed with m*CAT* transgenic mice (mouse with expression of human catalase gene in mitochondria; The Jackson Laboratory, stock #016197) to generate *Nox4 x* m*CAT* double transgenic mice. Mice were housed in ventilated cages at 22°C with a 12 h light/dark cycle, with free access to food and water and male mice were used in all the experiments.

VSMCs isolation and culture. Vascular smooth muscle cells (VSMCs) were isolated from aortas of 4 month-old wild-type, *Nox4TG*605 and *Nox4TG*618 male mice and cultured as described previously [12]. All experiments were performed using VSMCs that were growth arrested 72 h in DMEM supplemented with 0.1% FBS and were from passages 3–11.

Single cell gel electrophoresis (comet assay). Comet assay was performed using 1000 mouse VSMCs as described in *SI Materials and Methods*.

Mitochondrial DNA damage assay. VSMC mitochondrial DNA damage was assessed as described in *SI Materials and Methods*.

Immunofluorescence/Immunohistochemistry. DHE and MitoSOX Red fluorescence measurements for detection of superoxide and immunohistochemistry of VSMCs, mouse aortas, and human carotid arteries were performed as described previously [12] and in *SI Materials and Methods*.

BrdU incorporation assay. BrdU incorporation into VSMCs was performed as described in *SI Materials and Methods*.

SA-β-galactosidase assay. Senescence-associated β-gal staining in VSMCs was performed using cellular senescence staining kit (Cell Biolabs, Inc.) as described in *SI Materials and Methods*.

Amplex Red assay. H_2O_2 generation was measured using the Amplex® Red Hydrogen Peroxide Assay Kit (Invitrogen) as described previously [12] and in *SI Materials and Methods*.

Collagen gel contraction assay. Cell contraction was measured using a collagen gel based contraction assay kit (Cell Biolabs, Inc.) as described in *SI Materials and Methods*.

Mitochondrial bioenergetics assay. Mitochondrial bioenergetics were evaluated using the.

Seahorse XF-24 extracellular flux analyzer (Seahorse Biosciences) as described previously [12] and in *SI Materials and Methods*.

Analysis of cellular glycolysis. VSMC glycolysis levels were determined as described in *SI Materials and Methods*.

Citrate synthase activity assay. VSMC citrate synthase activity was analyzed as described in *SI Materials and Methods*.

Western blotting. Western blot analysis was performed as described previously [12] and in *SI Materials and Methods*.

Pulse wave velocity (PWV). PWV measurements were performed by the Physiology Phenotyping Core at the University of Michigan. The mice were anesthetized with 1–1.5% isoflurane/O_2 mixture to maintain a surgical plane of anesthesia and were placed on a warming pad to maintain body temperature at 37°C. ECG was monitored via non-invasive resting ECG electrodes. Pulse wave velocity between the thoracic and abdominal aorta was measured utilizing high temporal resolution of ECG-Gated Kilohertz Visualization (EKV) imaging using Visual Sonics Vevo 2100 high resolution *in vivo* micro-imaging system. Pulse wave velocity was calculated by dividing the arterial distance between these points, estimated using a measuring tape, and the time delay for the pulse, calculated based on the ECG.

3.1. Functional analysis of vascular reactivity

Wire myography. The vascular reactivity of aortic rings was analyzed by wire myography as described in *SI Materials and Methods.*

3.2. Determination of vascular mechanics

Pressure myography. Aortic stress-strain relationship and volume compliance were analyzed by pressure myography as described in *SI Materials and Methods.*

Focal adhesion turnover assay. VSMCs were grown to 60% confluence and were quiesced for 72 h in DMEM supplemented with 0.1% FBS. The cells were incubated with or without nocodazole (10 μM) for 2 h to depolymerize microtubules and thus dissolve the focal adhesions. The nocodazole was washed and cells were incubated in DMEM with 0.1% FBS to allow the reformation of focal adhesions for either 15 or 45 min. The cells were fixed with 4% paraformaldehyde and permeabilized with 0.05% Triton X-100. The cells were then stained for immunoreactive focal adhesion kinase (FAKpY397) primary antibody and an AlexaFluor secondary antibody to measure FAK specific immunofluorescence.

Measurement of VSMC stiffness with atomic force microscopy (AFM). AFM measurements of VSMC stiffness were performed by the Single Molecule Analysis in Real-Time (SMART) Center at the University of Michigan. AFM images and force-distance (F-D) traces were acquired on a TT-AFM (AFM Workshop, Signal Hill, CA) in contact mode in DMEM buffer with CSG01 probes (TipsNano, Tallinn, Estonia). Approximately 5–15 F-D curves were acquired per cell (serum-starved for 3 days), sampling many regions from each cell. AFM probe sensitivity was calibrated from F-D curves acquired on glass. Cantilever spring constant was estimated using the Sader method [69].

The F-D curves were fit assuming a pyramidal tip shape and a Poisson ratio of 0.5 to extract the Young's modulus using AtomicJ software [70]. The contact point of the F-D curve was estimated manually, and only the first 1 μm of deflection fit to estimate the stiffness of the cell without interference from the underlying glass substrate. Outliers more than 3 standard deviations above the mean were discarded.

Human carotid arteries. Human carotid artery segments were obtained through National Disease Research Interchange (NDRI). These samples were collected during autopsy 10–12 h postmortem. The postmortem subjects ranged in age from 21 to 89 years and included both male and female. The young subjects had an average age of 36.7 ± 6.28 (n = 18) and old 65.2 ± 12.8 (n = 46). All human carotid artery samples were deidentified and their use was approved by the University of Michigan Institutional Review Board. Samples from NDRI had incomplete medical history on comorbidities and prescription drugs.

Statistics. All biochemical experiments were conducted at least three times. Where applicable, 2-tailed Student's *t*-test was performed for significance. In other cases, where three groups are compared simultaneously, one-way ANOVA was performed with Bonferroni's post-hoc test. Differences were considered significant at $P < 0.05$.

Author contributions

C.C. and N.R.M. designed the study and experiments. C.C., M.D.S., A.E.V., J.R., and H.X. performed the experiments. T.H. performed mouse breeding. C.C., Y·Y.Z., D.T.E., M.S.R., and N.R.M. wrote the manuscript.

Disclosures

Dr. Marschall Runge is a member of the Board of Directors at Eli Lilly and Company.

Acknowledgements

This work was supported by a Pilot Grant (PG U063426) from University of Michigan Health System-Peking University Health Sciences Center Joint Institute for Translational and Clinical Research.

Appendix A. Supplementary data

Supplementary data to this article can be found online at https://doi.org/10.1016/j.redox.2019.101288.

References

[1] D.F. Dai, P.S. Rabinovitch, Z. Ungvari, Mitochondria and cardiovascular aging, Circ. Res. 110 (2012) 1109–1124.
[2] N.R. Madamanchi, M.S. Runge, Mitochondrial dysfunction in atherosclerosis, Circ. Res. 100 (2007) 460–473.
[3] S.J. Forrester, D.S. Kikuchi, M.S. Hernandes, Q. Xu, K.K. Griendling, Reactive oxygen species in metabolic and inflammatory signaling, Circ. Res. 122 (2018) 877–902.
[4] K. Bedard, K.H. Krause, The NOX family of ROS-generating NADPH oxidases: physiology and pathophysiology, Physiol. Rev. 87 (2007) 245–313.
[5] R.K. Ambasta, et al., Direct interaction of the novel Nox proteins with p22phox is required for the formation of a functionally active NADPH oxidase, J. Biol. Chem. 279 (2004) 45935–45941.
[6] A.N. Lyle, et al., Poldip2, a novel regulator of Nox4 and cytoskeletal integrity in vascular smooth muscle cells, Circ. Res. 105 (2009) 249–259.
[7] K.D. Martyn, L.M. Frederick, L.K. Von, M.C. Dinauer, U.G. Knaus, Function alanalysis of Nox4 reveals unique characteristics compared to other NADPH oxidases, Cell. Signal. 18 (2006) 69–82.
[8] L. Serrander, et al., NOX4 activity is determined by mRNA levels and reveals a unique pattern of ROS generation, Biochem. J. 406 (2007) 105–114.
[9] Y. Nisimoto, B.A. Diebold, D. Cosentino-Gomes, J.D. Lambeth, Nox4: a hydrogen peroxide-generating oxygen sensor, Biochemistry 53 (2014) 5111–5120.
[10] K. Block, Y. Gorin, H.E. Abboud, Subcellular localization of Nox4 and regulation in diabetes, Proc. Natl. Acad. Sci. U.S.A. 106 (2009) 14385–14390.
[11] T. Ago, et al., Upregulation of Nox4 by hypertrophic stimuli promotes apoptosis and mitochondrial dysfunction in cardiac myocytes, Circ. Res. 106 (2010) 1253–1264.
[12] A.E. Vendrov, et al., NOX4 NADPH oxidase-dependent mitochondrial oxidative stress in aging-associated cardiovascular disease, Antioxidants Redox Signal. 23 (2015) 1389–1409.
[13] F. Chen, S. Haigh, S. Barman, D.J. Fulton, From form to function: the role of Nox4 in the cardiovascular system, Front. Physiol. 3 (2012) 412.
[14] S. Lee, et al., A role for NADPH oxidase 4 in the activation of vascular endothelial cells by oxidized phospholipids, Free Radic. Biol. Med. 47 (2009) 145–151.
[15] A. Lozhkin, et al., NADPH oxidase 4 regulates vascular inflammation in aging and atherosclerosis, J. Mol. Cell. Cardiol. 102 (2017) 10–21.
[16] D. Sorescu, et al., Superoxide production and expression of Nox family proteins in human atherosclerosis, Circulation 105 (2002) 1429–1435.
[17] S. Laurent, et al., Aortic stiffness is an independent predictor of all-cause and cardiovascular mortality in hypertensive patients, Hypertension 3 (2001) 1236–1241.
[18] A. Sandoo, J.J. Van Zanten, G.S. Metsios, D. Carroll, G.D. Kitas, The endothelium and its role in regulating vascular tone, Open Cardiovasc. Med. J. 4 (2010) 302–312.
[19] W.W. Nichols, Clinical measurement of arterial stiffness obtained from noninvasive pressure waveforms, Am. J. Hypertens. 18 (2005) 3S–10S.
[20] B.M. Kaess, et al., Aortic stiffness, blood pressure progression, and incident hypertension, J. Am. Med. Assoc. 308 (2012) 875–881.
[21] J. Kals, et al., Inflammation and oxidative stress are associated differently with endothelial function and arterial stiffness in healthy subjects and in patients with atherosclerosis, Scand. J. Clin. Lab. Investig. 68 (2008) 594–601.
[22] R.H. Zhou, et al., Mitochondrial oxidative stress in aortic stiffening with age: the role of smooth muscle cell function, Arterioscler. Thromb. Vasc. Biol. 32 (2012) 745–755.
[23] T.J. LaRocca, C.M. Hearon Jr., G.D. Henson, D.R. Seals, Mitochondrial quality control and age-associated arterial stiffening, Exp. Gerontol. 58 (2014) 78–82.
[24] C. Schürmann, et al., The NADPH oxidase Nox4 has anti-atherosclerotic functions, Eur. Heart J. 36 (2015) 3447–3456.
[25] M. Zhang, et al., NADPH oxidase-4 mediates protection against chronic load-induced stress in mouse hearts by enhancing angiogenesis, Proc. Natl. Acad. Sci. U.S.A. 107 (2010) 18121–18126.
[26] X. Tong, et al., Pro-atherogenic role of smooth muscle Nox4-based NADPH oxidase, J. Mol. Cell. Cardiol. 92 (2016) 30–40.
[27] J. Kuroda, T. Ago, S. Matsushima, P. Zhai, M.D. Schneider, J. Sadoshima, NADPH oxidase 4 (Nox4) is a major source of oxidative stress in the failing heart, Proc. Natl. Acad. Sci. U.S.A. 107 (2010) 15565–15570.
[28] Q.D. Zhao, et al., NADPH oxidase 4 induces cardiac fibrosis and hypertrophy through activating Akt/mTOR and NFkappa B signaling pathways, Circulation 131 (2015) 643–655.
[29] C. Hirschhäuser, et al., NOX4 in mitochondria: yeast two-hybrid-based interaction with complex I without relevance for basal reactive oxygen species? Antioxidants Redox Signal. 23 (2015) 1106–1112.

[30] Y. Olgar, et al., Aging related functional and structural changes in the heart and aorta: MitoTEMPO improves aged-cardiovascular performance, Exp. Gerontol. 110 (2018) 172–181.
[31] J.B. Wheeler, R. Mukherjee, R.E. Stroud, J.A. Jones, J.S. Ikonomidis, Relation of murine thoracic aortic structural and cellular changes with aging to passive and active mechanical properties, J. Am. Heart Assoc. 4 (2015) e001744.
[32] H. Qiu, et al., Vascular smooth muscle cell stiffness as a mechanism for increased aortic stiffness with aging, Circ. Res. 107 (2010) 615–619.
[33] L. Jiang, et al., Calpain-1 regulation of matrix metalloproteinase 2 activity in vascular smooth muscle cells facilitates age-associated aortic wall calcification and fibrosis, Hypertension 60 (2012) 1192–1199.
[34] Y. Matsui, J. Sadoshima, Rapid upregulation of CTGF in cardiac myocytes by hypertrophic stimuli: implication for cardiac fibrosis and hypertrophy, J. Mol. Cell. Cardiol. 37 (2004) 477–481.
[35] J.C. Kohn, et al., Mechanical heterogeneities in the subendothelial matrix develop with age and decrease with exercise, J. Biomech. 49 (2016) 1447–1453.
[36] D. Hori, et al., miR-181b regulates vascular stiffness age dependently in part by regulating TGF-β signaling, PLoS One 12 (2017) e0174108.
[37] R.J. Saphirstein, et al., The focal adhesion: a regulated component of aortic stiffness, PLoS One 8 (2013) e62461.
[38] S.R. Datla, et al., Poldip2 controls vascular smooth muscle cell migration by regulating focal adhesion turnover and force polarization, Am. J. Physiol. Heart Circ. Physiol. 307 (2014) H945–H957.
[39] L. Kwong, M.A. Wozniak, A.S. Collins, S.D. Wilson, P.J. Keely, R-Ras promotes focal adhesion formation through focal adhesion kinase and p130(Cas) by a novel mechanism that differs from integrins, Mol. Cell. Biol. 23 (2003) 933–949.
[40] S.J. Zieman, V. Melenovsky, D.A. Kass, Mechanisms, pathophysiology, and therapy of arterial stiffness, Arterioscler. Thromb. Vasc. Biol. 25 (2005) 932–943.
[41] A.E. Vendrov, et al., NADPH oxidases regulate CD44 and hyaluronic acid expression in thrombin-treated vascular smooth muscle cells and in atherosclerosis, J. Biol. Chem. 285 (2010) 26545–26557.
[42] S. Chai, et al., Overexpression of hyaluronan in the tunica media promotes the development of atherosclerosis, Circ. Res. 96 (2005) 583–591.
[43] L.J. Niedernhofer, et al., Nuclear genomic instability and aging, Annu. Rev. Biochem. 87 (2018) 295–322.
[44] Z. Ungvari, G. Kaley, R. de Cabo, W.E. Sonntag, A. Csiszar, Mechanisms of vascular aging: new perspectives, J. Gerontol. A. Biol Sci. Med Sci. 65 (2010) 1028–1041.
[45] J. Kobayashi, Molecular mechanism of the recruitment of NBS1/hMRE11/hRAD50 complex to DNA double-strand breaks: NBS1 binds to gamma-H2AX through FHA/BRCT domain, J. Radiat. Res. 45 (2004) 473–478.
[46] A. Shah, et al., Defective base excision repair of oxidative DNA damage in vascular smooth muscle cells promotes atherosclerosis, Circulation 138 (2018) 1446–1462.
[47] D. Kang, S.H. Kim, N. Hamasaki, Mitochondrial transcription factor A (TFAM): roles in maintenance of mtDNA and cellular functions, Mitochondrion 7 (2007) 39–44.
[48] V.J. Bouchard, M. Rouleau, G.G. Poirier, PARP-1, a determinant of cell survival in response to DNA damage, Exp. Hematol. 31 (2003) 446–454.
[49] R. Colavitti, T. Finkel, Reactive oxygen species as mediators of cellular senescence, IUBMB Life 57 (2005) 277–281.
[50] B. Lener, et al., The NADPH oxidase Nox4 restricts the replicative lifespan of human endothelial cells, Biochem. J. 423 (2009) 363–374.
[51] N. Okita, S. Minato, E. Ohmi, S. Tanuma, Y. Higami, DNA damage-induced CHK1 autophosphorylation at Ser 296 is regulated by an intramolecular mechanism, FEBS Lett. 586 (2012) 3974–3979.
[52] D. Bacqueville, Phosphatidylinositol 3-kinase inhibitors block aortic smooth muscle cell proliferation in mid-late G1 phase: effect on cyclin-dependent kinase 2 and the inhibitory protein p27KIP1, Biochem. Biophys. Res. Commun. 244 (1998) 630–636.
[53] J. Wu, et al., Inflammation and mechanical stretch promote aortic stiffening in hypertension through activation of p38 mitogen-activated protein kinase, Circ. Res. 114 (2014) 616–625.
[54] P. Lacolley, P. Challande, M. Osborne-Pellegrin, V. Regnault, Genetics and pathophysiology of arterial stiffness, Cardiovasc. Res. 81 (2009) 637–648.
[55] M. Ferguson, R.J. Mockett, Y. Shen, W.C. Orr, R.S. Sohal, Age-associated decline in mitochondrial respiration and electron transport in Drosophila melanogaster, Biochem. J. 390 (2005) 501–511.
[56] D.F. Dai, et al., Overexpression of catalase targeted to mitochondria attenuates murine cardiac aging, Circulation 119 (2009) 2789–2797.
[57] R.A. Gioscia-Ryan, et al., Mitochondria-targeted antioxidant therapy with MitoQ ameliorates aortic stiffening in old mice, J. Appl. Physiol. 124 (1985) (2018) 1194–1202.
[58] M.J. Rossman, et al., Chronic supplementation with a mitochondrial antioxidant (MitoQ) improves vascular function in healthy older adults, Hypertension 71 (2018) 1056–1063.
[59] C.L. Berry, S.E. Greenwald, J.F. Rivett, Static mechanical properties of the developing and mature rat aorta, Cardiovasc. Res. 9 (1975) 669–678.
[60] Y.Z. Gao, R.J. Saphirstein, R. Yamin, B. Suki, K.G. Morgan, Aging impairs smooth muscle-mediated regulation of aortic stiffness: a defect in shock absorption function? Am. J. *Physiol. Heart Circ. Physiol.* 307 (2014) H1252–H1261.
[61] E. Crosas-Molist, T. Meirelles, J. López-Luque, C. Serra-Peinado, J. Selva, Vascular smooth muscle cell phenotypic changes in patients with Marfan syndrome, Arterioscler. Thromb. Vasc. Biol. 35 (2015) 960–972.
[62] B.S. Fleenor, K.D. Marshall, J.R. Durrant, L.A. Lesniewski, D.R. Seals, Arterial stiffening with ageing is associated with transforming growth factor-β1-related changes in adventitial collagen: reversal by aerobic exercise, J. Physiol. 588 (2010) 3971–3982.
[63] Y. Shen, M.D. Schaller, Focal adhesion targeting: the critical determinant of FAK regulation and substrate phosphorylation, Mol. Biol. Cell 10 (1999) 2507–2518.
[64] D. Zhang, et al., Mitochondrial cardiomyopathy caused by elevated reactive oxygen species and impaired cardiomyocyte proliferation, Circ. Res. 122 (2018) 74–87.
[65] G. Ji, et al., MiR-146a regulates SOD2 expression in H_2O_2 stimulated PC12 cells, PLoS One 8 (2013) e69351.
[66] A. Dregan, Arterial stiffness association with chronic inflammatory disorders in the UK Biobank study, Heart 104 (2018) 1257–1262.
[67] J. Wu, et al., Inflammation and mechanical stretch promote aortic stiffening in hypertension through activation of p38 mitogen-activated protein kinase, Circ. Res. 114 (2014) 616–625.
[68] H.T. Yu, et al., Arterial stiffness is associated with cytomegalovirus-specific senescent $CD8_+$ T cells, J. Am. Heart Assoc. 6 (2017) pii: e006535.
[69] J.E. Sader, J.W.M. Chon, P. Mulvaney, Calibration of rectangular atomic force microscope cantilevers, Rev. Sci. Instrum. 70 (1999) 3967–3969.
[70] P. Hermanowicz, M. Sarna, K. Burda, H. Gabryś, AtomicJ: an open source software for analysis of force curves, Rev. Sci. Instrum. 85 (2014) 063703.